2

Conf-910739--26

PNL-SA--18880

DE91 015531

0-G EXPERIMENTS WITH ADVANCED CERAMIC FABRIC WICK STRUCTURES

Z. I. Antoniak
B. J. Webb
J. M. Bates
M. F. Cooper
K. A. Pauley

July 1991

Presented at the
1991 National Heat Transfer Conference
July 28-31, 1991
Minneapolis, Minnesota

Work supported by
the U.S. Department of Energy
under Contract DE-AC06-76RLO 1830

Pacific Northwest Laboratory
Richland, Washington 99352

DISCLAIMER

TESTING OF ADVANCED CERAMIC FABRIC WICK STRUCTURES AND THEIR USE IN A WATER HEAT PIPE

Zenen I. Antoniak, Brent J. Webb, James M. Bates, Matthew F. Cooper, and Keith A. Pauley
Energy Sciences Department
Pacific Northwest Laboratory
Richland, WA 99352
(509)375-3841

ABSTRACT

A prototype ceramic fabric/titanium water heat pipe has been constructed and tested; it transported up to 60 W of power at about 390 K. Startup and operation both with and against gravity were examined. Wick testing was begun to aid in the design and construction of an improved prototype heat pipe, with a 38-μm stainless steel liner covered by a biaxially-braided Nextel (trademark of the 3M Co., St. Paul, Minnesota) sleeve that is approximately 300-μm thick. Wick testing took place in 1-g; limited testing in 0-g was initiated, and results to-date suggest that in 0-g, wick performance improves over that in 1-g.

INTRODUCTION

Both Air Force and NASA future spacecraft thermal management needs span the temperature range from cryogenics to liquid metals. Many of these needs are changing and not well defined and will remain so until goals, technology, and missions converge. Nevertheless, it is certain that high-temperature (> 800 K) and medium-temperature (about 450 K) radiator systems will have to be developed that offer significant improvements over current designs. This paper discusses experiments performed in the lower temperature regime as part of a comprehensive advanced ceramic fabric (ACF) heat pipe development program. These experiments encompassed wicking tests with various ceramic fabric samples, and heat transfer tests with a 1-m long prototype ACF water heat pipe.

WICKING TESTS

Background

The development of ACF heat pipes requires a thorough understanding of the operation and optimization of various subcomponents. One important area of research is the utilization of ACF materials as wick structures. These structures have been tested by the Pacific Northwest Laboratory (PNL) in both 1- g and 0-g environments.

A typical ACF water heat pipe is constructed with an outer ACF structural sheath, an impermeable metal liner material, and an inner ACF wicking structure. Working fluid pressure seats the thin liner material against the outer ACF layer, and the resulting liner corrugation may be useful as a limited wick primarily in the circumferential direction (Antoniak et al. 1989). ACF arteries may also be added to the heat pipe design for further optimization. A schematic diagram of a heat pipe constructed of ACF materials is illustrated in figure 1.

A literature review was performed, but few relevant references were found on 0-g wick performance. PNL investigated the feasibility of electroplating samples of Nextel fabric with copper and nickel for possible use as wicks. The nickel coatings showed good adherence to the fabric, and were applied in thin layers without rigidizing the fabric. The copper coated samples did not adhere as well to the fabric, and had a tendency to flake off. To improve adherence copper coating thickness was increased, but only at the expense of rigidizing the fabric. Coated fabric samples were not tested as wicks, but additional work in this area is suggested.

Theoretical Background

The PNL fluid wicking experiment was designed to procure information necessary for the design of efficient heat pipes for space applications. The primary data required is the effective pumping radius, r_p, of the ACF wicking materials when operating in 0-g. This pumping radius can be determined from the relationship:

$$r_p = \frac{4t_a K\sigma\cos\theta}{\mu_l \varepsilon x_a^2} \quad (1)$$

where t_a is the time to reach point x_a, K is the permeability, μ_l is the dynamic viscosity of the liquid, and ε is the porosity (see Figure 2) (Brennan and Kroliczek 1979).

Experimental Apparatus

The 0-g fluid wicking apparatus, shown in Figure 3, is constructed in three parts: a sample ribbon, an actuation device, and a redundant sensor module. Fabric wicking samples are mounted on a 3.81 cm wide mylar strip. The mylar strip and samples are initially rolled onto a supply reel. One end of the mylar is fed through the sensing window and attached to a take-up reel. The samples are then moved into the sensing window individually by a hand lever attached to the take-up reel.

When a sample is positioned into the sensing window, a hand lever is turned, rotating a cam which brings a liquid reservoir filled with sponge material into contact with the sample. The sample is clamped between the sponge material protruding from an opening in the reservoir and a plate on the other side of the sample. The experiment for this sample is terminated by simply backing the liquid reservoir away from the sample. A new sample may then be positioned into the window.

Twenty different samples were placed on the mylar carrier strip. These samples consisted of four different types of fabrics (about 375 μm thick) and one type of sleeving (about 0.003 m dia.) placed in different geometries. The geometries used were: flat fabric with both sides exposed to air, double layers of flat fabrics with both sides exposed to air, and flat fabrics stitched to corrugated aluminum foil. Table1 lists the combination of materials and configurations utilized.

The samples that used flat fabric were placed over windows cut into the mylar and fastened around the edges of the window. This allowed the wicking to take place in the fabric alone without being disturbed by contact with any other surfaces and allowed the use of the electro-optic sensors described below. The samples were approximately one inch wide and six inches long.

An array of electro-optic sensors was placed along the side of the sensing window. Each of these sensors consisted of an LED and photodetector in one integral unit. The LED and photodetector were mounted on opposite sides of a slot approximately 0.0048 m wide. When a flat fabric sample was rolled into the sensing window, the edge of the fabric was positioned in the slot between the LED and photodetector. When the fabric becomes wet, the transmittance changes, and the change is detectable by sensing a change in the resistance across the photodetector. With an array of these sensors along the wicking path it was possible to measure the time when the wicking front arrived at each sensor. The speed of the wicking front could then be inferred from this data.

In addition to the electro-optic sensors, an array of thermocouples was also attached to the structure that holds the liquid reservoir. When the liquid reservoir is moved into contact with the sample, the thermocouples simultaneously contact the back of the sample. As the wicking front arrived at a thermocouple, the change in temperature from a dry-bulb to a wet-bulb condition was detected.

The third sensing method was a visual record of the experiment taken by a video camera. The samples were lit from the side opposite the camera by a diffuse, fluorescent light source. The wicking front was visible as a small change in the transmittance of the fabric.

TABLE 1. Fluid Wicking Sample Material and Configuration.

Sample Number	Description
1	Nextel 440 Flat Fabric/Plain Weave
2	Astroquartz Flat Fabric/Plain Weave
3	Nextel 312 Flat Fabric/Plain Weave
4	Nextel 440 Tape/Woven
5	Nextel 440 Sleeving/Nextel 440 Thread Fill
6	Nextel 440 Sleeving/Nextel 312 Thread Fill
7	Nextel 440 Sleeving/Kao-Wool Fill
8	Nextel 440 Sleeving/Empty
9	Same as 1 but double layer
10	Same as 3 but double layer
11	Same as 2 but double layer
12	Filter Paper standard
13	Nextel 312 Flat Fabric/Corrugated Al Foil
14	Nextel 440 Flat Fabric/Corrugated Al Foil
15	Astroquartz Flat Fabric/Corrugated Al Foil
16	Nextel 440 Tape/Corrugated Al Foil
17	Same as 6 but mounted on Nextel 440 Fabric
18	Same as 5 but mounted on Nextel 440 Fabric
19	Same as 7 but mounted on Nextel 440 Fabric
20	Same as 8 but mounted on Nextel 440 Fabric

Test Results

1-G Testing. Extensive ground testing was conducted on the fluid wicking apparatus both before and after the reduced-gravity experimentation on the NASA KC-135 plane. These tests were performed in both vertical and horizontal configurations. At this time analyses has not been completed on the large amount of data gathered in this test.

0-G Testing. Two days of reduced-gravity testing were performed with the PNL fluid wicking apparatus on the NASA KC-135 plane. The same set of test samples was flown both days in order to attempt to generate reproducible results.

The data generated on these flights is limited due to equipment problems during the first day of testing. After about six reduced-gravity parabolas, a power spike destroyed the electro-optical sensor array and shut down the data acquisition computer which contained the previously acquired data in its RAM. The thermocouple technique functioned poorly in the humid south Texas environment, principally due to the small difference between the dry- and wet-bulb temperatures. Therefore, the only valid data from the 0-g wicking tests is extracted from the video camera record, which is sometimes difficult to interpret. The wicking front could be observed for only the first five samples shown in Table 1. Figure 4 provides preliminary results of the wicking test for the these five samples for 1-g vertical and horizontal conditions, and the data obtained during the two days of 0-g flight testing. The error in this data is on the order of 0.001 m/s. It appears that the wicking improves in 0-g; it is theorized that performance in a horizontal 1-g position is lower because of meniscus recession into the wick, and resulting wick effective area reduction. We intend to repeat these experiments, using better and more reliable sensing techniques with pure (undyed) fluids as before.

ACF HEAT PIPE TESTING

A non-optimized prototype ACF heat pipe was built using currently-available materials. It was constructed as follows:

• Outer liner	430-μm (17-mil) thick biaxially-braided Nextel fabric
• Metal liner	200-μm (8-mil) titanium alloy
• Wick	ca. 250-μm (10-mil) Nextel, held in place with 100-mesh stainless steel screen
• End fittings	standard Swagelok
• Working fluid	water
• Dimensions	titanium is 0.016-m (5/8-in) OD x 0.9-m (36-in) long
• evaporator	0.229-m (9-in) (wrapped with electrical heating tape)
• adiabatic section	0.15 m
• condenser	Heat rejection is to ambient air.

Instrumentation consisted of type J thermocouples placed on the outside of the fabric along the condenser, and sandwiched between the heating tape and insulation at the evaporator; also, a pressure transducer was mounted on the condenser end of the heat pipe (see Figure 5). Data acquisition was automated via a microcomputer adapted with appropriate hardware and software. The thermocouple error is estimated to be about 2 K, and the pressure transducer error is < 25 kPa (4 psi).

Initial performance measurements indicated lower power throughput, and reduced condenser temperatures and operating length when the heat pipe was operated against gravity. More recently, we have been able to obtain improved performance at negative tilt angles, with near-constant condenser temperature (see Figure 6). This improvement was achieved by further cleaning of the wick, plus addition of 10 - 15 cc of water after the wick was fully saturated. This heat pipe was then operated with 60 W heat input. Heat throughput is estimated to be 10 - 20 W lower. Startup at negative tilt is readily achieved (see Figures 7 and 8).

We have also been able to maintain constant heat input, from horizontal to slight negative tilt of - 5 degrees , although temperature at the evaporator does increase by about 12 degrees (see Figure 9). Code predictions (Woloshun et al. 1988) confirm that this is a reasonable level of performance to expect.

ACKNOWLEDGMENTS

This work was performed by Pacific Northwest Laboratory and has been supported by the Department of Energy, Richland Operations Office; the National Aeronautics and Space Administration (Lewis and Johnson Research Centers); and the Air Force (Astronautics and Weapons Laboratories). Pacific Northwest Laboratory is operated for the U. S. Department of Energy by Battelle Memorial Institute.

REFERENCES

Antoniak, Z. I., Bates, J. M., and Webb, B. J., 1989, "Design of Ceramic Fabric Heat Pipe with Water Working Fluid," Proceedings, 26th National Heat Transfer Conference, S. B. Yilmaz, ed., American Institute of Chemical Engineers, New York, NY, pp. 230-234.

Brennan, P. J., and Kroliczek, E. J., 1979, Heat Pipe Design Handbook, B & K Engineering, Inc., Towson, MD, pp. 116-169, 280-287.

Woloshun, K. A., Merrigan, M. A., and Best, E. D., 1988, HTPIPE: A Steady-State Heat Pipe Analysis Program, LA-11324-M, Los Alamos National Laboratory, Los Alamos, NM.

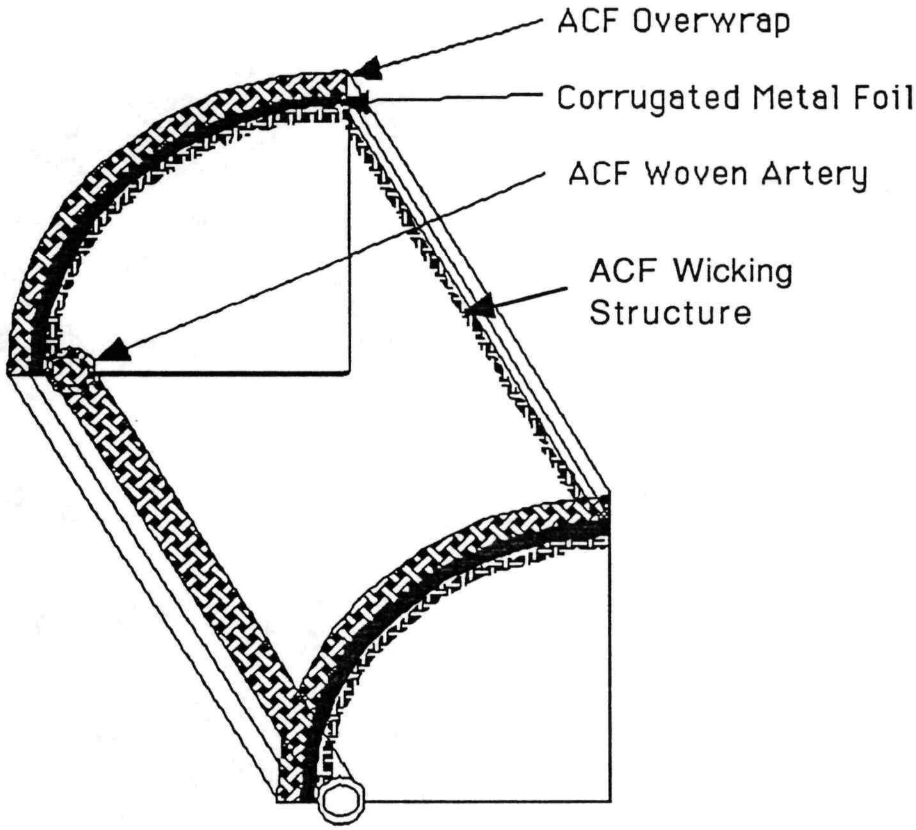

Figure 1. ACF Heat Pipe Cross-section.

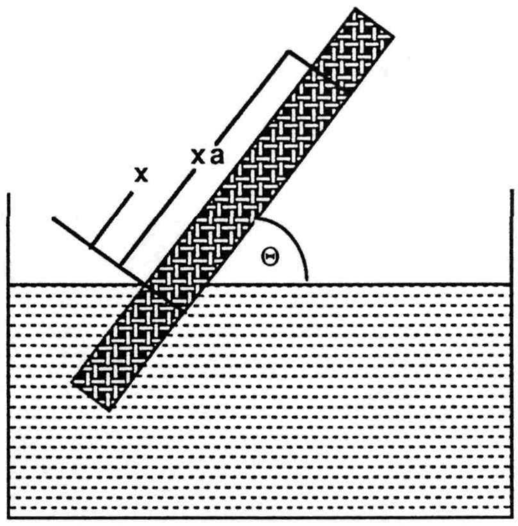

Figure 2. Geometry for Pore Radius Calculation.

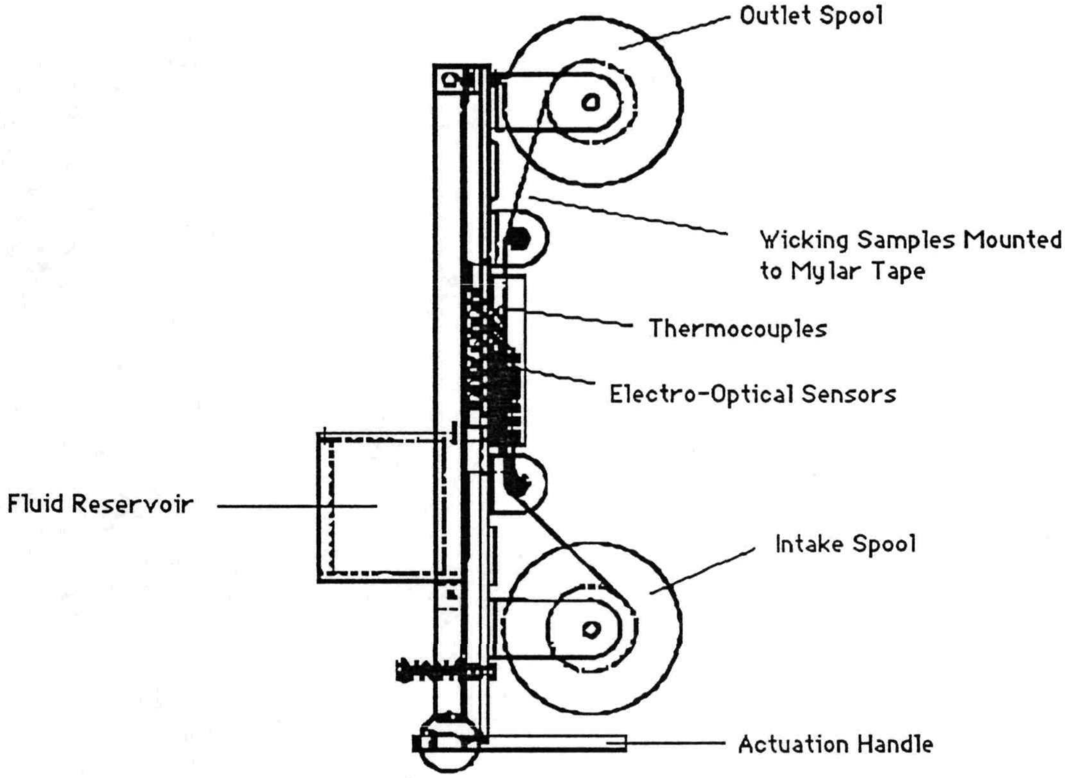

FIGURE 3. 0-g Fluid Wicking Apparatus.

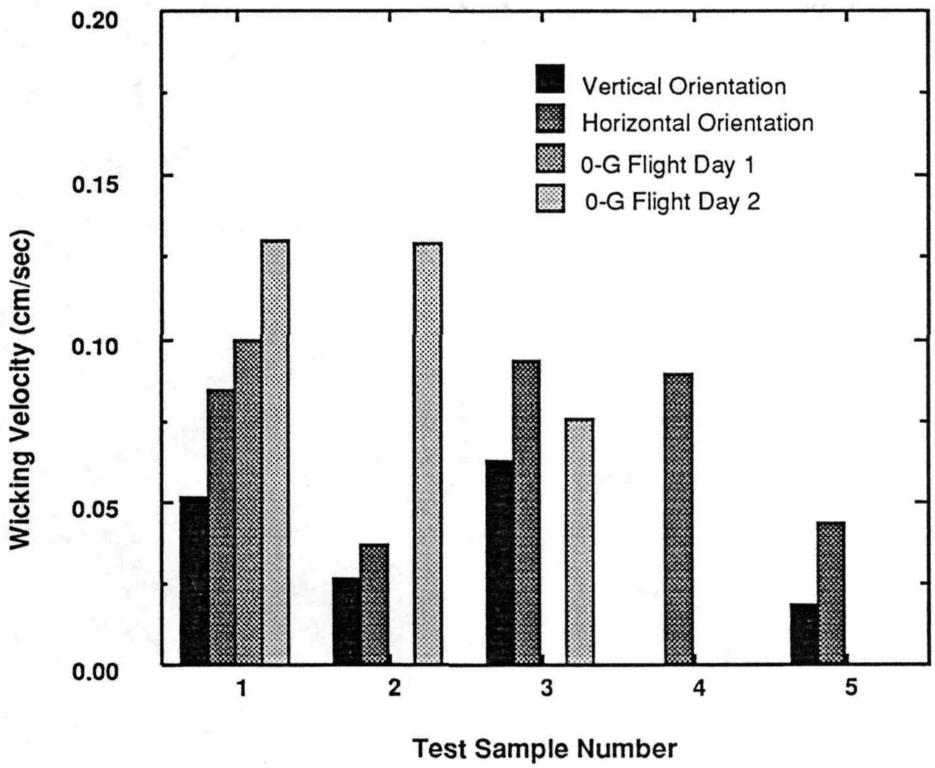

FIGURE 4. Preliminary Results of Wicking Tests.

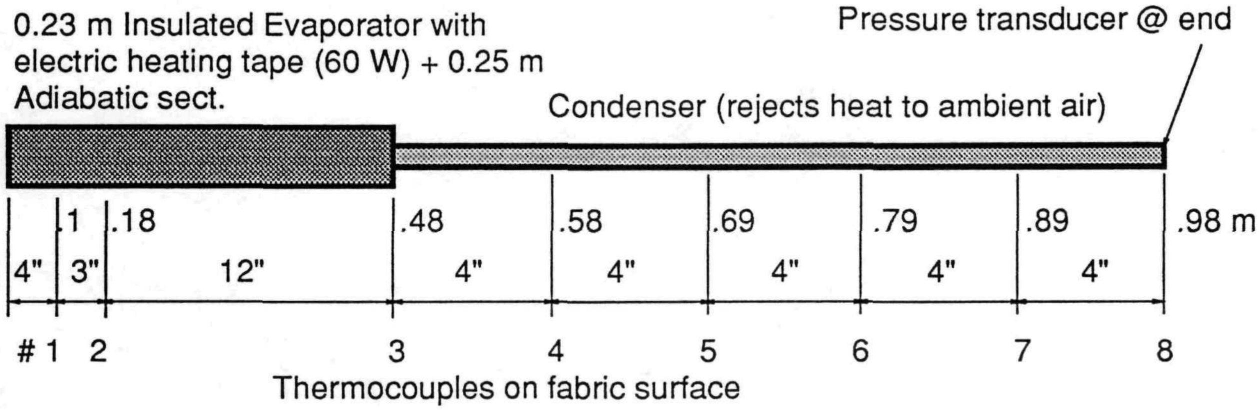

Figure 5. Arrangement of Test ACF Water Heat Pipe.

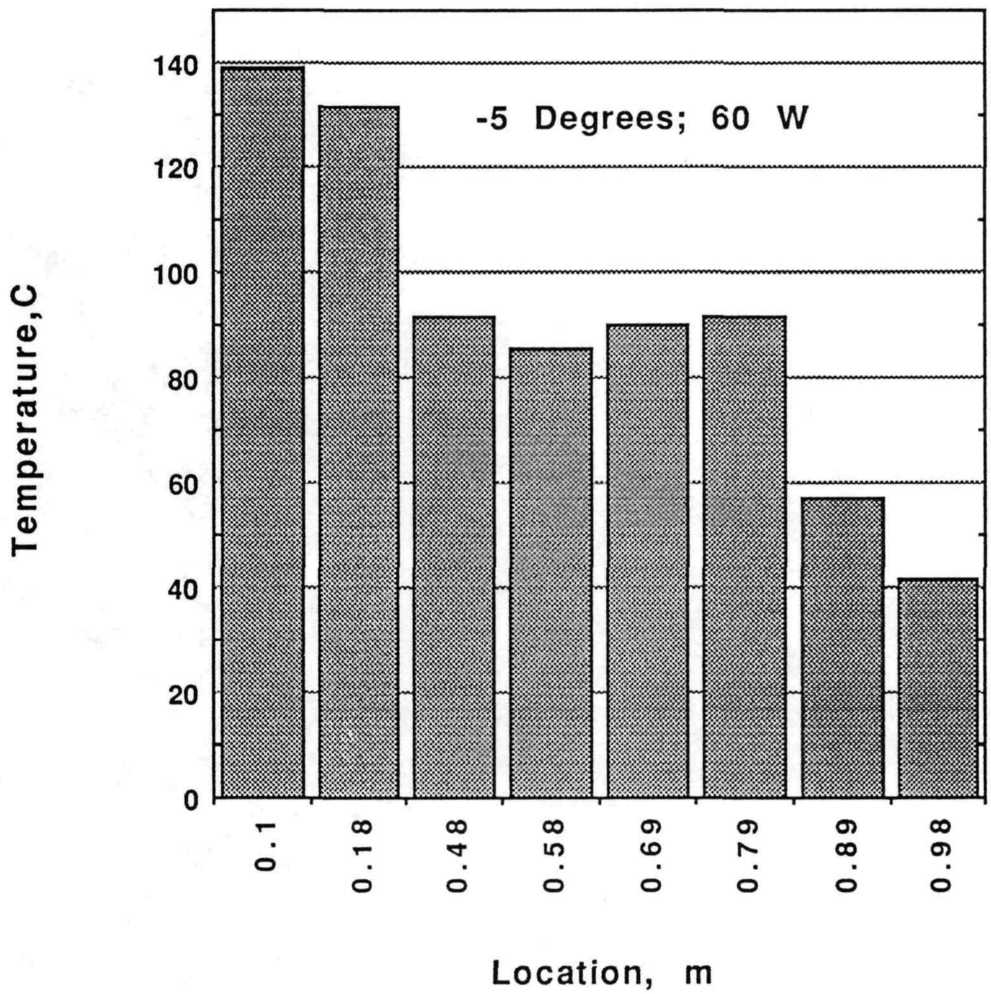

Figure 6. ACF Heat Pipe Axial Temperature Profile at Steady-State.

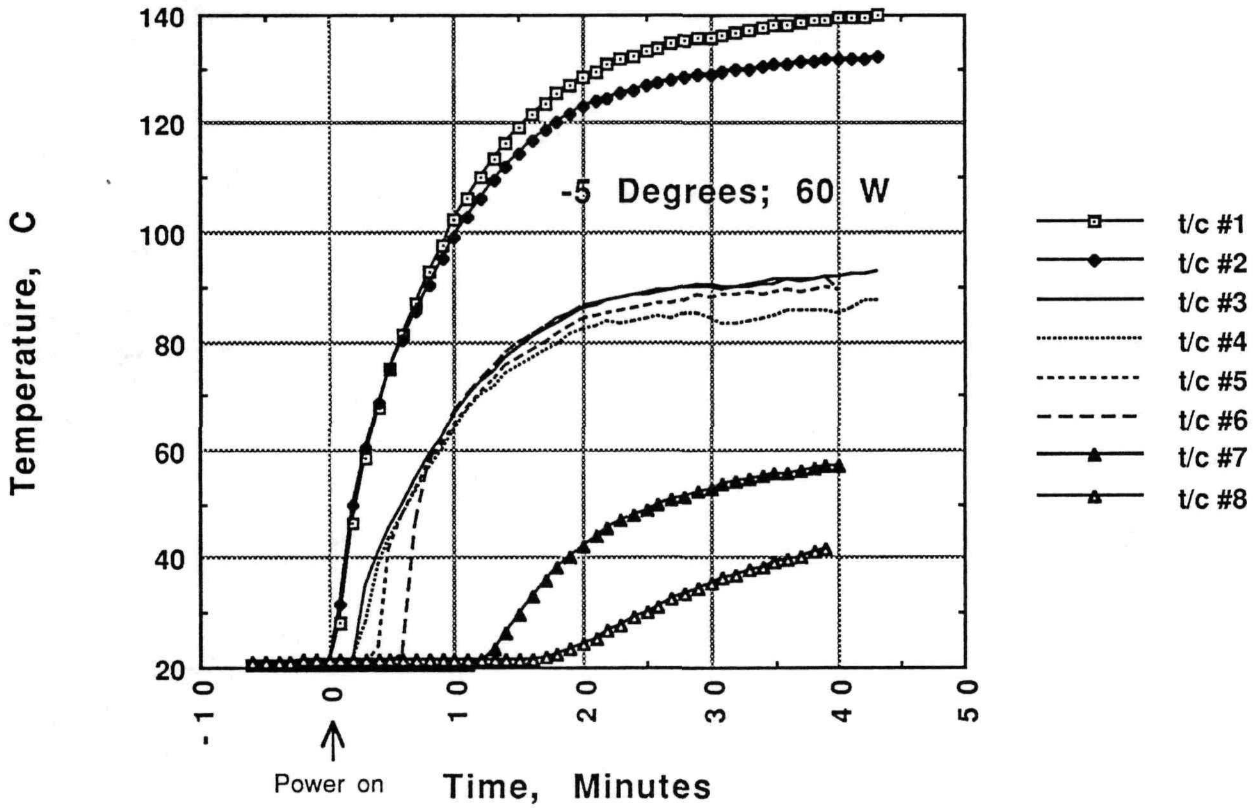

Figure 7. ACF Heat Pipe Startup Transient.

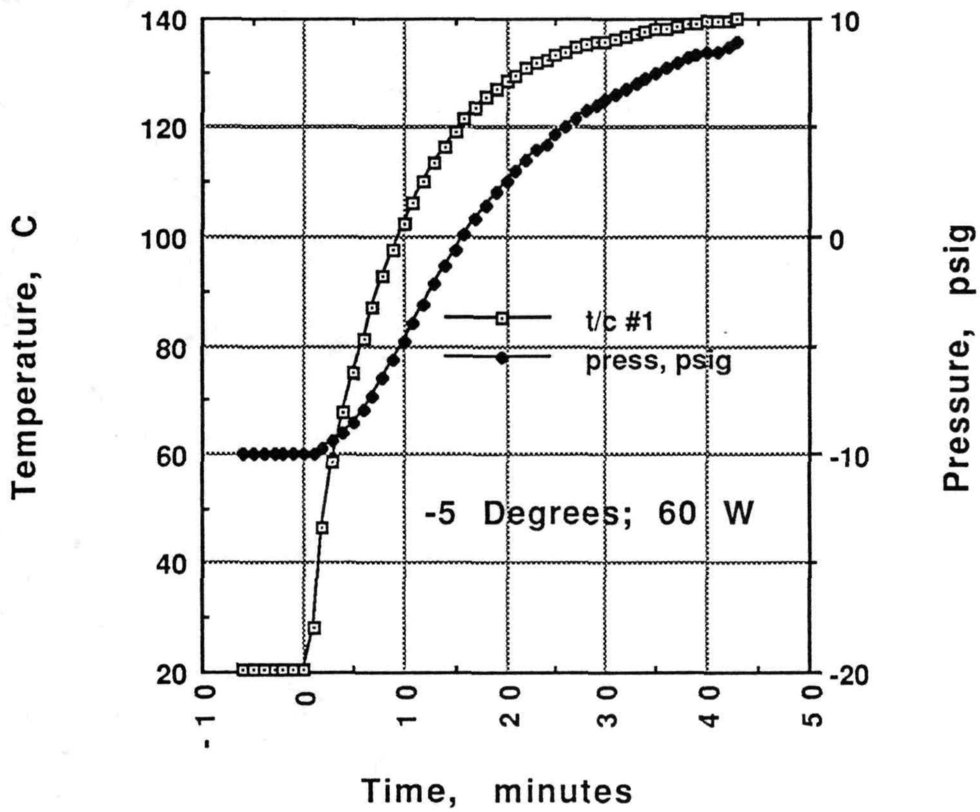

Figure 8. ACF Heat Pipe Startup Transient Temperature and Pressure.

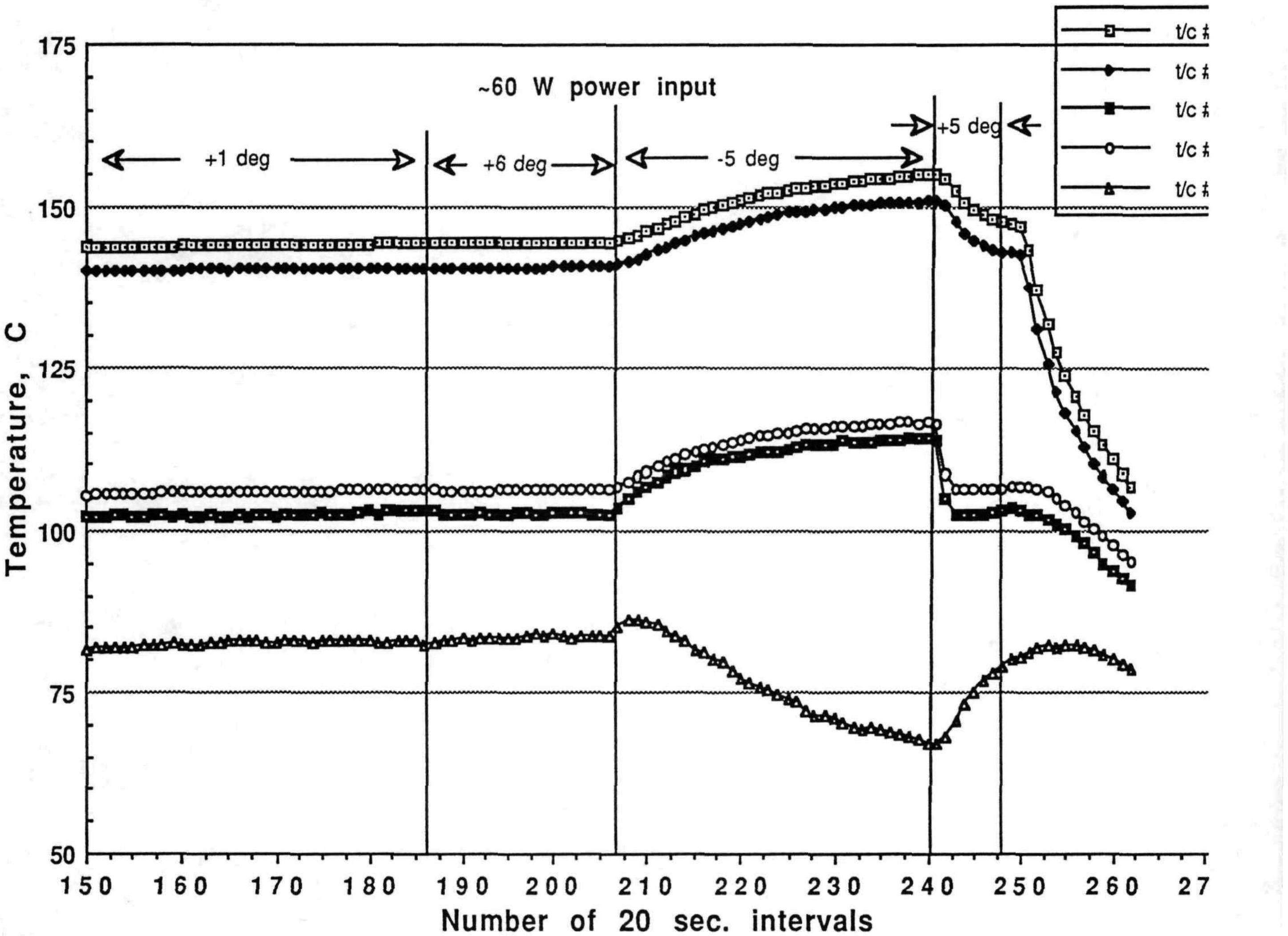

Figure 9. ACF Heat Pipe Test of Sensitivity to Orientation.